The impact of climate change on riverine flooding

Albert J. Kettner[1], Sagy Cohen[2], Irina Overeem[1], Balazs M. Fekete[3], G. Robert Brakenridge[1], James P.M. Syvitski[1]

[1)] Dartmouth Flood Observatory (DFO), Community Surface Dynamics Modeling System (CSDMS), Institute of Arctic and Alpine Research (INSTAAR), University of Colorado, Boulder CO, USA; [2)] University of Alabama, Tuscaloosa, AL, USA; [3)] The City University of New York, Dep. of Civil Engineering, NY, USA.

Kettner@colorado.edu

This project (Global flood risk from advanced modeling and remote sensing in collaboration with Google Earth Engine) is funded by National Aeronautics and Space Administration, NASA, AIST program under award number: NNX15AG85G.

Introduction

Flooding is the most common natural hazard worldwide, affecting 21 million people every year. Flood risk contributes to a global-average annual loss of US$104 billion (UNISDR, 2015). These losses are expected to increase as the economic value of material assets in flood prone zones is expected to rise due to growth in population and wealth (Jongman et al., 2012; Winsemius, et al., 2015). While some events are seasonal in nature, large floods are episodic making flooding difficult to predict. Recent advances in modeling of river-floodplain interactions do provide first order estimates of the magnitude, frequency, and duration of floods of global rivers. In this study we focus on expected changes in river flood discharges due to climate change by the end of the 21st century. Socio-economic impacts are not considered, nor do we analyze changes in areal extent of floods. We focus our analysis on changes over the period of flood discharges that we define as discharges larger than the bankfull, with a 2-year recurrence interval using a daily time step. This recurrence interval is slightly more conservative than the 1.5-year flow event, which is used to determine bankfull stage of a river (e.g. Simon et al., 2004). Daily global simulations of water discharge over a 30-year period are used to establish bankfull discharge as well as other flood recurrence intervals. We employ a simulated climate scenario for 2070-2099, forced by a moderate Representative Concentration Pathway (RCP 4.5), as input for a global water balance model. Than the Water Balance Model (WBMplus) is applied to quantify: a) location, frequency and magnitude of flooding, and b) the impact of future climate change on these characteristics.

Methods

Model

To study the impact of climate change on flood characteristics we apply the fully coupled Water Balance Model (WBMplus) (Vörösmarty et al. 1989; Wisser et al., 2008; 2010). The model incorporates natural hydrological processes (i.e. precipitation, snow accumulation and melt; evaporation; groundwater storage and release) as well as engineering measures (i.e. diversion of riverine water for irrigation, water storage in reservoirs) that influence river hydrographs. Our simulations use a global grid with a spatial resolution of 6 arc-minutes (~11 by 11 km at the equator) (Vörösmarty et al. 2000). To isolate the impacts of climate change on flood characteristics, no other model input parameters were altered.

Climate Scenarios

We use the climatology of the Hadley Global Environment Model 2, HadGEM2-ESv2 (Martin et al., 2011), with historical forcing and a representative concentration pathway (RCP 4.5) as input for the WBMplus model for 30-y time periods of interest, 1975-2004 and 2070-2099. We choose to use a conservative RCP forcing (RCP4.5) (Clarke et al., 2007). This scenario assumes total radiative forcing will be stabilized before 2100 by implementation of a range of technologies for reducing greenhouse gas emissions. This climate simulation has a moderate climate warming projection with an average of 1.8 °C (range of 1.1 to 2.6 °C) by 2100. It is 'moderate' compared to other CMIPS5 climate scenarios like RCP2.6, which has an optimistic minimal temperature increase by 2100 of on average 1.0°C, ranging between 0.3 to 1.7 °C) or the more extreme RCP8.5 with an average temperature increase of 3.7 by 2100 and a range of 2.6 to 4.8 °C.

Applied methods to determine recurrence intervals for river reaches globally

We use daily numerical simulations from the WBMplus model for a 30-year period, 1975-2004 to calculate recurrence intervals. Recurrence intervals are determined by establishing a Log-Pearson Type III distribution for each grid cell for the model output. Applying the Log-Pearson Type III method is recommended to estimate water discharge recurrence intervals (IACWD, 1982), and has become common practice. For each grid cell, we compute the log mean discharge (eq. 2), its standard deviation (eq. 3) and the skewness coefficient (eq. 4) to determine the logarithmic water discharge (log Q) for a certain recurrence interval (eq. 1) following Bedient and Huber (2002)

Eq. 1: $$log\,Q = \overline{Log\,Q} + K\sigma_{Log\,Q}$$

Eq. 2: $$\overline{Log\,Q} = \mathrm{E}\,(Log\,Q_i)\,/\,n$$

Eq. 3: $$\sigma_{log\,Q} = (log\,Q_i - (\overline{log\,Q})^2/(n-1))^{0.5}$$

Eq. 4: $$Cs = \frac{n\,\mathrm{E}\,(log\,Q_i - \overline{Log\,Q})^3}{(n-1)(n-2)(\sigma_{log\,Q})^3}$$

where Qi is the annual peak discharge (m3/s); and n the number of simulated years (-), 30 in this specific case. The frequency factor K is a function of the skewness coefficient Cs (eq. 4) and the recurrence interval of interest.

We analyze the model output, consisting of a 30-year global daily dataset for 1975-2004, to determine the number of times daily discharge at any given reach would exceed a certain recurrence interval. To identify the impact of 21st century climate conditions on flood magnitude and frequency, we use the same set of discharge recurrence intervals established from the 20th century data, and applied those threshold to count the number of times daily discharge exceeds these thresholds for the 21st century climate conditions.

Figure 1 illustrates this methodology for the Yukon River in Arctic Alaska. We compare the WBMplus modeled discharge daily time series for 1974-2004 to observed data at Pilot Station, AK, and calculate bankfull and respective flood recurrence intervals based on these time series. Whereas modeled river discharges for this particular site are systematically slightly less than observed discharge, the pattern of the obtained recurrence intervals matches well (Panel A). Figure 1C and D contrast the floodplain dynamics of the Yukon River at bankfull conditions on 06/18/2003, with 05/24/2009 one of the highest spring discharges in the last 35 years. Model predictions point to a decline of the common 2-5 year flood discharges, and an increase of moderate events (both 5-10 year and 10-25 year recurrence intervals) for this particular river system (Figure 1B).

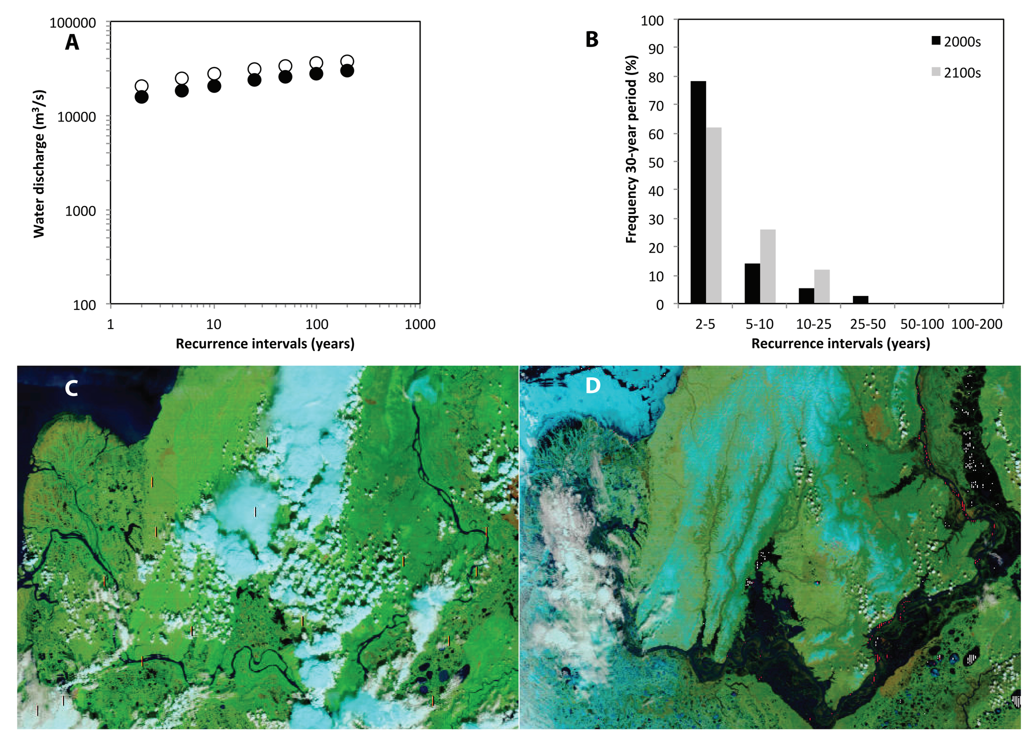

Figure 1. Yukon River near its delta in Arctic Alaska. A) Recurrence intervals with associated peak water discharge for observed discharge (open dots) and simulated discharges (solid dots) estimated using a Log-Pearson Type III distribution for the Yukon River at Pilot Station (61°56'04", 162°52'50"); B) the frequency of each recurrence interval for the 2000s (black) and 2100s (grey) at that same location; C) Approximately banfull conditions for the Yukon River during June 2003; and D) flooding with a recurrence interval between 25-50year at that same location during May 2009.

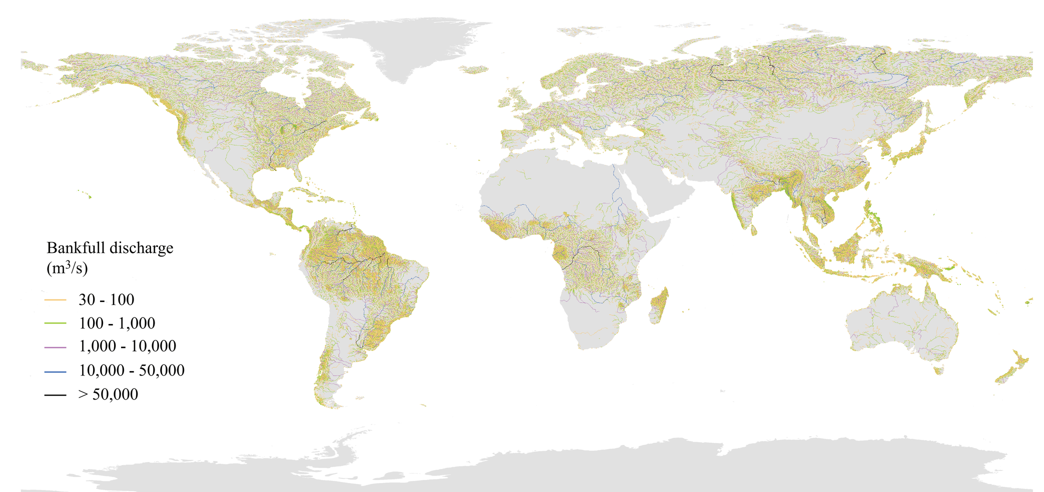

Figure 2. The 2-year recurrence interval as established from a Log-Pearson III distribution based on 30-year daily-simulated global water discharge defines the 'bankfull discharge'. Bankfull discharge less than 30 m³/s (grey areas) are not taken into consideration.

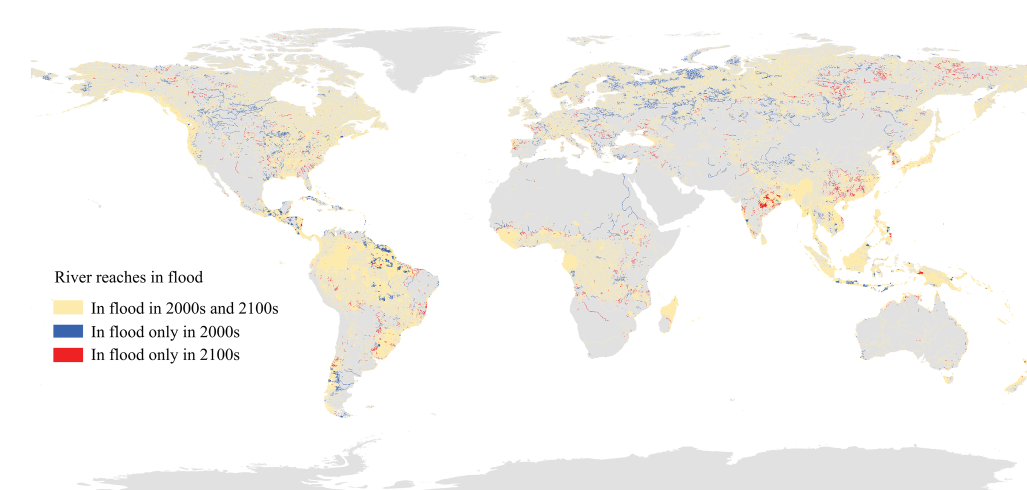

Figure 3. Simulated flooded river reaches for a flood discharge larger than 10year flood recurrence interval in the 2000s and 2100s.

Results

Discharge recurrence intervals are estimated using the daily global WBMplus simulations over a 30-year period (1975-2004). Bankfull discharge is globally established by assigning a two-year recurrence interval discharge to each river segment, where bankfull discharges are larger than 30 m3/s (Figure 2). Rivers with a bankfull discharge of less than 30 m3/s, like rivers located in the Sahara desert, the Middle East, Tibetan plateau, large parts of inland Australia and the American Rocky Mountains are not considered in this study..

Using the calculated recurrence interval discharges based on the end of the 20th century climate regime, we investigate whether there is a spatial difference in flooded river segments in the 2100s. Figure 3 shows the distribution of river reaches that were modeled to flood in a 30year period with water discharge larger than the 10-year recurrence interval for the 2000s and for the 2100s. Notice that large regions of the Midwest of North America as well as Europe and west Asia will not exceed at least a 10-year recurrence interval flood in the 2100s anymore (Figure 3, blue areas). Similarly, many river reaches of northeast India and East Asia will newly experience floods of at least a 10-year recurrence interval in the 2100s (Figure 3, red areas).

Flood frequency for the range of flood recurrence intervals for the 2000s and the 2100s is calculated by counting the number of days water discharge of each river reach is larger than the specific recurrence discharge magnitude. We define the 'percentage change in flood frequency for a specific flood magnitude' as the difference in this calculated flood frequency between 2000s and 2100s. Percentage flood frequency difference for discharges at least larger than the bankfull recurrence interval are shown in figure 4A. Notably, the map indicates that the flood frequency for the smaller floods is reduced for the Midwest of North America, Europe and West Asia, but also for the north east of South America, and many parts of southwest Indonesia for the 2100s (Figure 4A, red areas). Simulations indicate that flood frequency of similar floods will increase for many river reaches in the Eastern part of North America, Alaska, northwestern part of South America, middle Africa, and south Asia. A rather similar pattern occurs for the change in flood frequency of extreme floods, i.e. larger than the 100year recurrence interval (Figure 4B).

When analyzing the flood frequency changes per continent, the percentage change in flood frequency for each recurrence interval increases for all continents by 2100s, with the exception of Europe (Table 1). According to our model simulation Europe will see a decrease of 22% for the smaller floods (5-10 year recurrence interval), and an 8% decrease for moderate flood discharges (10-25 year recurrence interval. Also, the most extreme flood discharges increase significantly for all continents, most by close to 200% or more.

Table 1. Percentage change in estimated flood frequency per recurrence interval per continent, comparing 2000s – 2100s. Negative values indicate an expected decrease in flooding.

	Percentage change in flood frequency per recurrence interval (years)				
Continent	**5 - 10**	**10 - 25**	**25 - 50**	**50 - 100**	**100 - 200**
Africa	42	70	106	152	182
Asia	74	106	144	180	219
Australia	46	67	106	176	302
Europe	-22	-8	14	27	39
North America	30	74	131	174	229
South America	80	126	176	227	261
World	*52*	*87*	*130*	*169*	*208*

Although the frequency of flood discharges increases significantly for almost all continents, for the medium to larger floods (recurrence intervals between 10-25, 25-50 and 50-100 years) the percentage of local-river reaches that, according to our simulations, experience flood discharges are actually decreasing by 2100s, (Table 2). Although for the smaller floods with a 5-10 year recurrence interval, more river reaches will experience small flood discharges.

Table 2. Percentage change in river reaches affected by flooding per flood magnitude per continent, comparing 2000s - 2100s. Negative values indicate an expected decrease in the number of flooded reaches.

	Percentage change in river stretches affected by flooding per flood recurrence interval (years)				
Continent	**5 - 10**	**10 - 25**	**25 - 50**	**50 - 100**	**100 - 200**
Africa	-4	-45	-42	-16	-11
Asia	0	-31	-32	-12	17
Australia	-6	-36	-25	17	103
Europe	107	-16	-32	-23	-10
North America	32	-40	-41	-26	6
South America	18	-42	-38	-10	23
World	*18*	*-35*	*-36*	*-16*	*10*

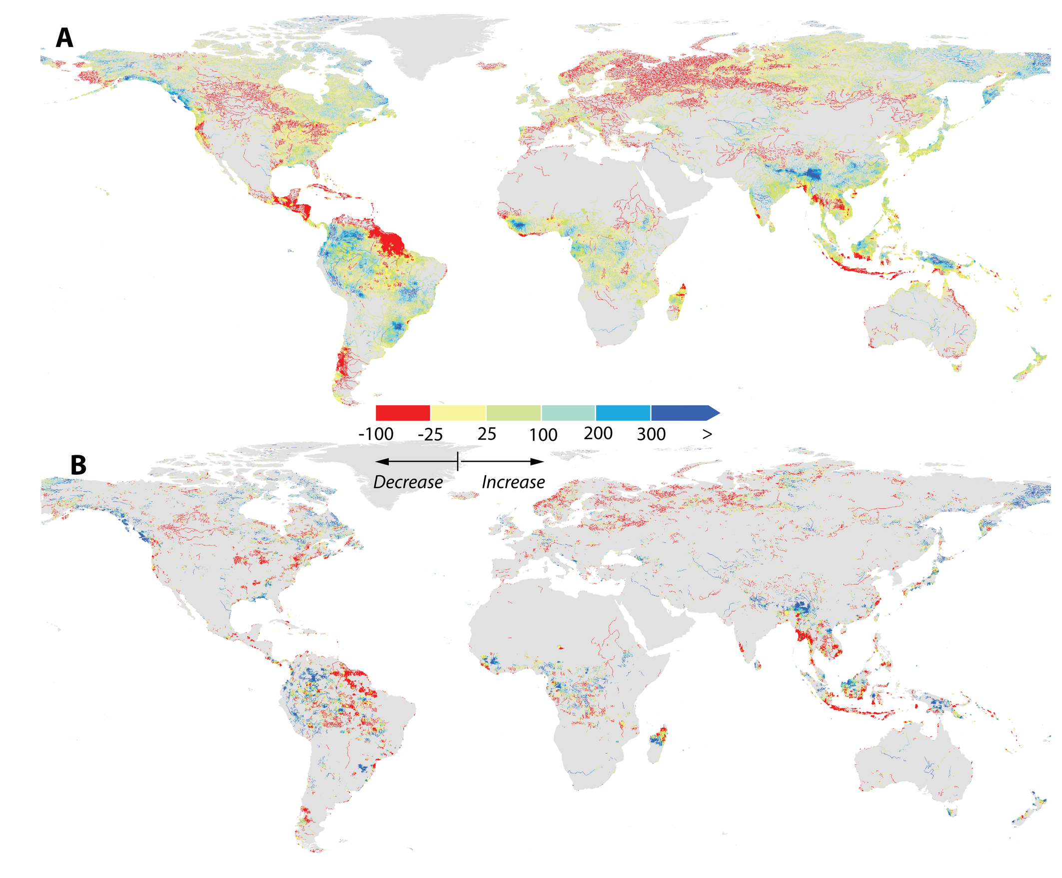

Figure 4. Spatial representation of percentage change flood frequency between the 2000s and 2100s for all floods that have: A) a larger than the bankfull (2-y) recurrence interval, and B) larger than 100-y recurrence interval.

Conclusions

Towards the end of the 21st century: overall a decrease in the percentage of river reaches that are affected by flooding for moderate to larger recurrence intervals (10–100 year).

For the smaller recurrence intervals (5-10 years) and the much larger return periods (100-200 year) an opposite trend was observed: increased flooding towards the end of the 21st century.

Flood frequencies will increase significantly for all continents by the end of the 21st century. Europe is the exception where we observed a reduced flood frequency for the lower recurrence intervals (5-25 year).

References

Bedient, P.B., and Huber, W.C., 2002. Hydrology and Floodplain Analysis. Prentice-Hall, Inc., Upper Saddle River, 763 p.
Clarke, L., Edmonds, J., Jacoby, H., Pitcher, H., Reilly, J., and Richels, R., 2007. Scenarios of greenhouse gas emissions and atmospheric concentrations, report, 154 pp., U.S. Clim. Change Sci. Program, Washington, D. C.
Interagency Advisory Committee on Water Data (IACWD), 1982. Guidelines for determining flood flow frequency. Bulletin 17B of the Hydrology Subcommittee OWDC, US Geological Survey, Reston, VA.
Jongman, B., Ward, P.J., and Aerts, J.C.J.H., 2012. Global exposure to river and coastal flooding: Long term trends and changes. Global Environmental Change, 22, 823-835. Doi: 10.1016/j.gloenvcha.2012.07.004.
Martin, G.M., et al., 2011. The HadGEM2 family of Met Office Unified Model climate configurations, Geosci. Model Dev., 4, 723-757. Doi: 10.5194/gmd-4-723-2011.
Simon, A., Dickerson, W., and Heins, A., 2004. Suspended-sediment transport rates at the 1.5-year recurrence interval for ecoregions of the United States: transport conditions at the bankfull and effective discharge? Geomorphology, 58, 243-262. Doi: 10.1016/j.geomorph.2003.07.003.
UNISDR (2015). Making Development Sustainable: The Future of Disaster Risk Management. Global Assessment Report on Disaster Risk Reduction. Geneva, Switzerland: United Nations Office for Disaster Risk Reduction (UNISDR).
Vörösmarty, C.J., Moore III, B., Grace, A.L., and Gildea, M.P., 1989. Continental scale models of water balance and fluvial transport: an application to South America. Global Biogeochemical cycles, 3, 241-265. Doi: 10.1029/GB003i003p00241.
Vörösmarty, C.J., Fekete, B.M., Meybeck, M., and Lammers, R.B., 2000. Geomorphometric attributes of the global system of rivers at 30-minute spatial resolution. J. Hydrol., 237 (1–2) (2000), pp. 17–39. doi: 10.1016/s0022-1694(00)00282-1.
Wisser, D., Frolking, S., Douglas, E.M., Fekete, B.M., Vörösmarty, C.J., and Schumann, A.H., 2008. Global irrigation water demand: variability and uncertainties arising from agricultural and climate data sets. Geophysical Research Letters, 35.
Wisser, D., Fekete, B.M., Vörösmarty, C.J., and Schumann, A.H., 2010. Reconstructing 20th century global hydrography: a contribution to the Global Terrestrial Network – Hydrology (GTN-H). Hydrology and Earth System Sciences, 14, 1-24.
Winsemius, H.C., Aerts, J.C.J.H., van Beek, L.P.H., Bierkens, M.F.P., Bouwman, A., Jongman, B., Kwadijk, J.C.J., Ligtvoet, W., Lucas, P.L., van Vuuren, D.P., and Ward, P.J., 2015. Global drivers of future river flood risk. Nature Climate Change. Doi: 10.1038/nclimate2893.